

A FLEXIBLE WAY TO REFLECT ON THE UNIVERSE

The W.M. Keck Observatory telescopes on Hawaii are receiving upgrades that include an Adaptive Secondary Mirror (ASM) and the Keck Wide Field Imager (KWFI). The upgrade is accompanied by an ambitious proposal to implement a deployment mechanism. This system will enable rapid switching between the ASM and KWFI within the limited available space, and unlock their full potential. This article discusses the design considerations for the work, commissioned by TNO as a graduation project.

BAS HUISMAN

Introduction

As part of “Keck 2035”, the W.M. Keck Observatory, home to two of the world’s most advanced optical telescopes, is set to receive a major upgrade in the coming years [1]. Built in the 1980s, these 10-meter-class telescopes, Keck I and II, have been at the forefront of infrared astronomy for decades. Rather than replacing them with a new system, the plan is to enhance their capabilities with state-of-the-art technology.

Two of the significant upgrades are concerned with the optics at the primal focus of the telescope. First, large-scale adaptive optics will be introduced. While Keck II already features adaptive optics on a small scale, the goal is to implement a large Adaptive Secondary Mirror (ASM). Incorporating adaptive optics at this early stage in the light path and on such a scale is expected to provide a substantial performance boost. A second upgrade is the Keck Wide Field Imager (KWFI), a new instrument designed for wide-field infrared observations. With a 1° field of view of the celestial dome, it will be ideal for scanning the sky for unpredicted cosmic phenomena. Unlike the ASM, the KWFI directly collects light from the primary mirror without reflecting it back into the telescope.

A key design challenge is that both the proposed 1.4-meter-diameter ASM and the KWFI must occupy approximately

the same location in the telescope: the spider structure where the current secondary optical element is mounted (highlighted in blue in Figure 1). While Keck I and II can exchange instrument carriages (yellow) at this position, the process takes several hours and can only be performed outside of observation hours. Consequently, only one of the proposed instruments can be used per observation night.

Ideally, both proposed instruments should be operational during a single observation night to fully utilise their capabilities. This would require a single carriage featuring both instruments, with the ASM being retractable to allow direct light from the primary mirror to reach the KWFI. Figure 2 illustrates the light paths in both the retracted (Figure 2a) and the deployed (Figure 2b) configuration.

Despite strong interest in such a system, it has long been considered impractical due to the limited space available within the carriage. This scepticism was further fuelled by the implementation of the retractable M3, which has revealed significant challenges in achieving the required deployment repeatability [2].

While the KWFI is being developed externally at the University of California, Santa Cruz [3], TNO aimed to win the contract to develop the stationary ASM. To strengthen their bidding position, a detailed study by means of a CAD validation model

AUTHOR’S NOTE

Bas Huisman studied Mechanical Engineering at Eindhoven University of Technology in Eindhoven (NL), where he is now a Ph.D. candidate in the Design for Precision Engineering research group. This article features the deployable mechanism that he designed for TNO, as described in his M.Sc. thesis [4], which earned him a nomination for the Wim van der Hoek Award 2024.

b.huisman@tue.nl

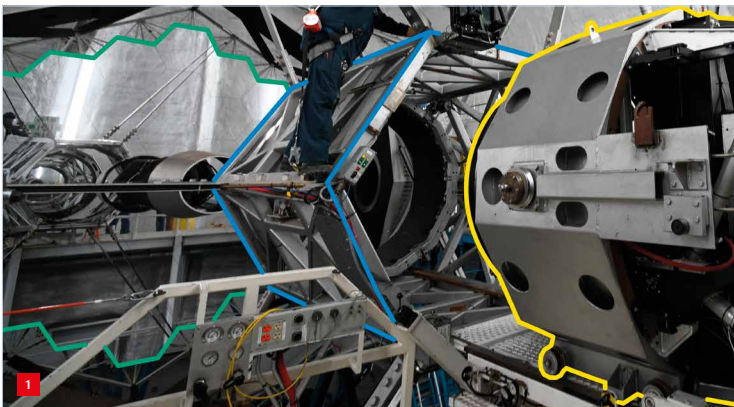
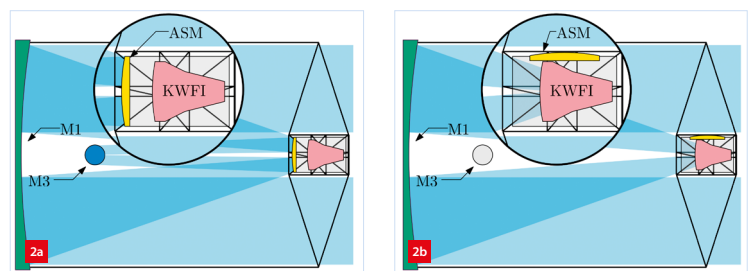
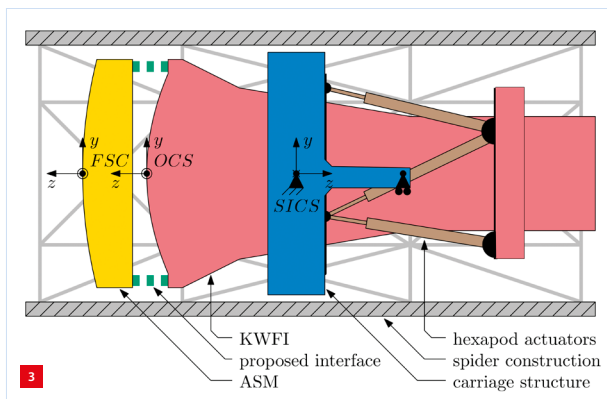


Photo taken during loading of the F/15 Secondary Mirror carriage (yellow) into the spider structure (blue). In the background, the segmented primary mirror is outlined in green. (Image courtesy of Fred Kamphues, TNO)



Schematic representation of the light path within the Keck telescopes. (a) Telescope in ASM mode. (b) Telescope in KWFI mode.



Schematic overview of significant components within the proposed carriage (blue) configuration, including KWFI (red), ASM (yellow), hexapod (brown) and proposed interface (green).

was required concerning the feasibility of incorporating the ‘moonshot’ desired deployability of the ASM.

The main challenges in this design stemmed from the limited available design space, the varying gravity direction due to telescope movement, and the very strict positional stability requirements on the ASM, regardless of the telescope-elevation angle. This article presents some of the interesting design details [4]. Although one of the interesting topics, limited information will be provided regarding the mechanism providing highly accurate and repeatable deployment, because of confidentiality.

Spatial challenges

Challenges arose due to both the ASM and KWFI occupying roughly the same space and the tight spider construction. Figure 3 provides a cross-sectional side view of this spider structure, previously introduced in Figure 1. The blue structure represents the carriage, which serves as the inter-

face between the spider structure, at the Spider Interface Coordinate System (SICS), and any instrument mounted within. Leaving this interface unchanged is crucial for backward compatibility of legacy instruments.

Inside the carriage, the KWFI (red) and ASM (yellow) are shown in their required observational positions. The Origin Coordinate System (OCS) origin is defined as the centroid of the anterior lens of the KWFI. The Face Sheet Centroid (FSC) of the adaptive mirror has its own coordinate system, which moves with the ASM. As the KWFI requires minor positional adjustments during observation, it is mounted on a 6-DoF (degree of freedom) hexapod (brown). This hexapod also proves beneficial for aligning the ASM, as explained in the text box, leading to the decision to have the ASM interface with the KWFI rather than directly with the carriage structure – a choice further driven by space constraints. The green dotted lines indicate this, to be developed, interface.

Alignment and deformation compensation

The entire structure of the telescope deforms due to gravity, temperature and other load variations. Tables mapping this deformation are already available. Using the hexapod introduced in Figure 3 as an actuator, an open-loop control system will be used to keep the KWFI at the compensated position.

The ASM is part of an adaptive optics loop, which can also be used to close the hexapod correction loop. This will significantly reduce the repeatability and stability requirements on the deployment mechanism. Unfortunately, many observations will use the ASM in passive mode, making this way of closing the loop not universally applicable.

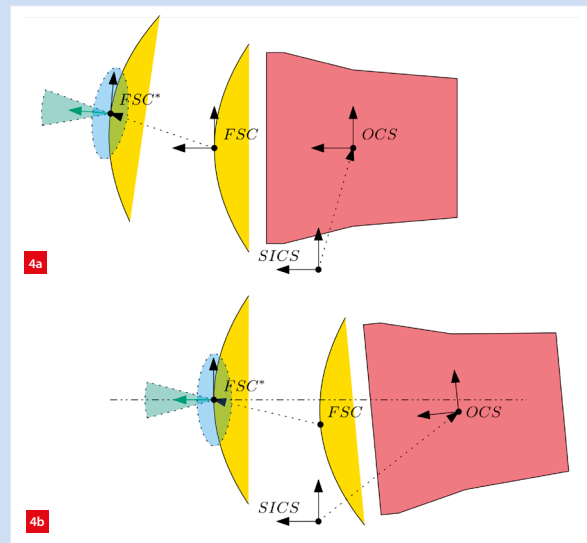
There are plans for a calibration sequence, using a Phase Shifting Camera (PSC), to calibrate the ASM position. This camera can measure the actual pre-focus position (FSC*, Figure 4a) within a certain range. Using the hexapod, the entire system can then be adjusted until FSC* coincides with the required FSC position (Figure 4b). As this sequence is time-consuming, it will be performed only once a day.

However, predictable elastic and thermal deformations can be compensated. It is assumed that elastic displacement errors due to elevation changes are expected to be reduced to 5% of their original values, while for thermal errors this is 10%. > continue on next page

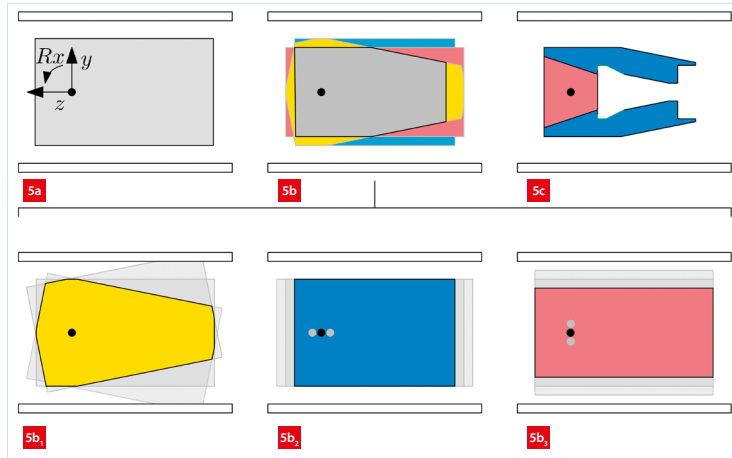
Abbreviations

ASM	Adaptive Secondary Mirror
CG	Centre of Gravity
DoF	Degree of Freedom
KWFI	Keck Wide Field Imager
FSC	Face Sheet Centroid
GCS	Global Coordinate System
MRA	Mirror Rotation Axis
OCS	Origin Coordinate System
PSC	Phase Shifting Camera
PWCA	Pneumatic Weight Compensation Actuator
RBE3	Rigid Body Element type 3
SICS	Spider Interface Coordinate System
TC	Thermal Centre
TBSA	Telescopic Ball-Screw Actuator

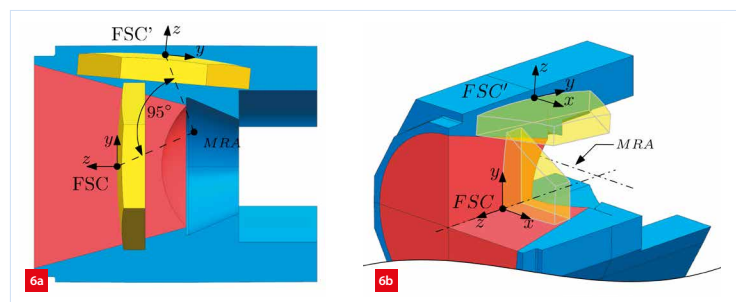
Concluding on the above-mentioned arguments, the time during which the stability requirement of the system must be held, is reduced to a single night’s observation. Furthermore, the deployment repeatability (order of single-digit microns in the z -direction) is most critical as in between deployments no calibration is possible. In the final part of this article, a table concerning the repeatability requirements and estimated performance is presented. Repeatability is not further elaborated upon, because of confidentiality.



Schematic representation of the calibration sequence. (a) Measurement using the PSC within the spatial (blue) and angular (green) tolerance. (b) Position of the FSC after the focus event, executed by the hexapod.



2D representation of the steps undertaken to define the available design space. (a) Maximum stationary design space. (b) Grey: design space build-up. (b₁) Yellow: overlapping area of design space allowed at each R_x . (b₂) Blue: overlapping area of design space allowed at each T_z . (b₃) Red: overlapping area of design space allowed at each T_y . (c) Red: KWFI light path (must be cleared when retracted); blue: design space available at each configuration of the mechanism.



CAD model of the chosen deployed and retracted position of the ASM. (a) Side view, indicating the rotational path the mirror undergoes. (b) Trimetric view, providing a better understanding of the position within the design space.

This architecture results in both the ASM and KWFI moving within the spider structure, reducing the available design space. Figure 5 illustrates the constraints in 2D. In Figure 5a, the grey block is defined by maintaining a 20-mm safety clearance from the spider structure (white). Figure 5b reduces this volume by considering this clearance at each maximum rotation (Figure 5b₁) and all translations (Figures 5b₂ and 5b₃). Further constraints arose from the KWFI and carriage geometry, defining the final design space in Figure 5c. The blue area represents space that is always available, while the red area cannot be used in ASM-retracted mode, as it corresponds to the KWFI light cone.

With the design space and operational positions of both the KWFI and ASM established, the next challenge is to find the ASM’s ideal retracted position. The thickness of the ASM is a critical factor, as a thicker design will improve bending stiffness, increasing its first internal eigenmode. Conclusively, maximising allowable thickness becomes the key criterion for selecting a retraction position.

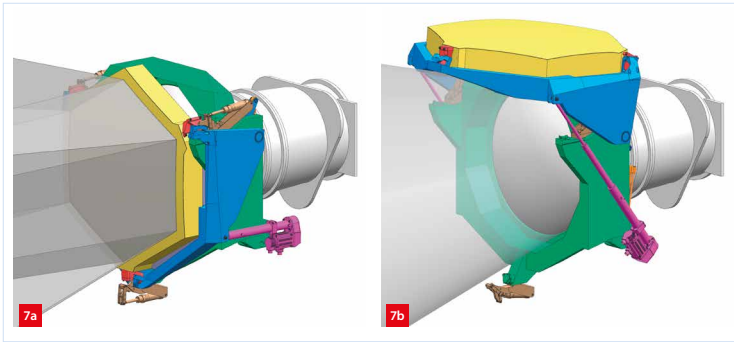
Figure 6a illustrates a retraction position that enables an ASM assembly thickness of 228 mm. This position is accessible via

a 95° pure rotation around the Mirror Rotation Axis (MRA). The 3D trimetric view in Figure 6b confirms that the ASM remains within the design space (blue + red) when deployed and clears the KWFI light cone (red) when retracted.

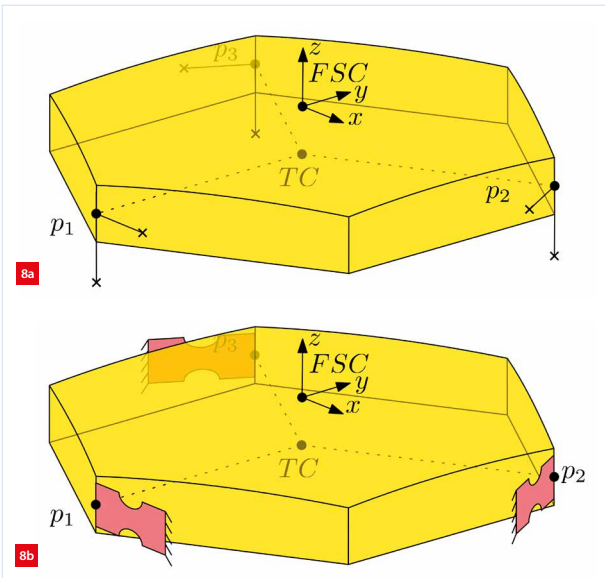
Design details

The final validation model of the deployable ASM concept is shown both deployed and retracted in Figures 7a and 7b, respectively. Figure 7a shows the ASM (yellow) mounted to the base structure (green) at three positions, positioned 120° around the mirror, with elastic elements (red). When retracted (in Figure 7b), it is shown that the mirror, and its three flexible elements, is held by the deployment structure (blue) and is moved out of the way. Between the green, blue and red parts, a clever interface is present ensuring maximal deployment repeatability. This article does not delve deeper into this interface, because of the aforementioned confidentiality.

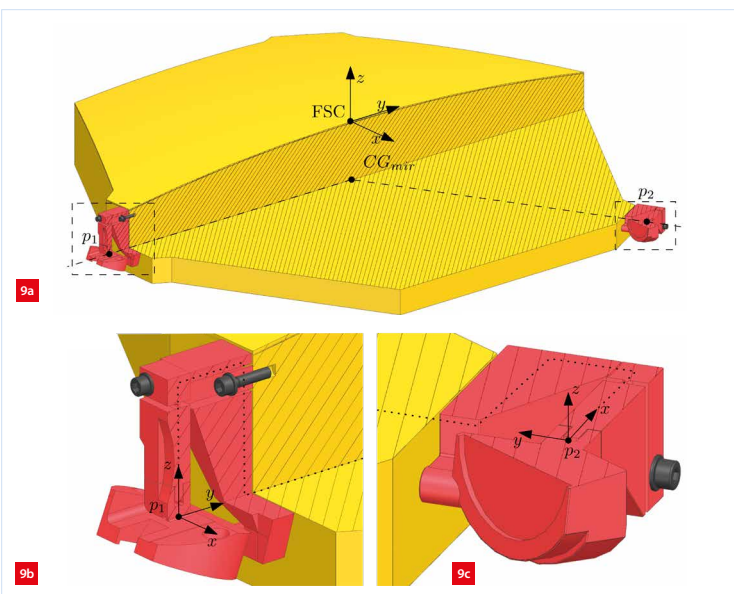
Various other aspects of the design, however, can be discussed in detail. This concerns the mirror mounting using the flexible



CAD render of the final validation model.
 (a) The deployed configuration, including the reflective light path.
 (b) The retracted configuration, including the KWFI light path.



Schematic view of ASM holding positions; TC is the Thermal Centre.
 (a) Including the FSC coordinate system.
 (b) Including a schematic representation of the proposed flexure equivalent constraint.



Section cut view of flexible mirror support.
 (a) Overview, including mirror points p_1 , p_2 and the Centre of Gravity (CG).
 (b) Detailed view of the flexible element at p_1 , showing the force path as a dotted line.
 (c) Detailed view of the flexible element at p_2 , showing the force path as a dotted line.

elements, the welded plate structures, and the actuation of the deployment including a pneumatic weight-compensation system.

Holding the mirror

Given the significant temperature fluctuations atop Maunakea, designing a thermally stable, exactly constrained mirror mount is critical. Various exactly constrained solutions featuring a Thermal Centre (TC) along the z -axis of the FSC have been considered. Eventually, the solution shown in Figure 8a is selected, because of its symmetry and the highest resulting first eigenmode of the mirror it holds. This solution constrains the mirror at three positions in two DoFs, spaced evenly at 120° around the mirror.

Next, it is considered what elements can be used to decouple the DoFs at each of these positions. At first, kinematic couplings such as V-grooves, or Canoe-spheres in Maxwell configuration, are considered [5]. However, these are rejected, due to the risk of their friction influencing the shape of the mirror during thermal cycling. The chosen solution uses elastic elements, as they lack this friction.

Figure 9 shows the implementation of this solution in the validation model. Each of the three flexible elements constrains two DoFs, which in the final validation model is implemented using wire-EDM-machined components from Ti6Al4V, indicated in red in Figures 9b and 9c. Note that the centres of rotation of the flexible elements form a plane that coincides with the centre of mass of the mirror.

The ends of the wire-EDM-machined components are rigidly connected to either the green Base Structure, or the blue Deployment Structure (Figure 7), dependent on the current state of deployment.

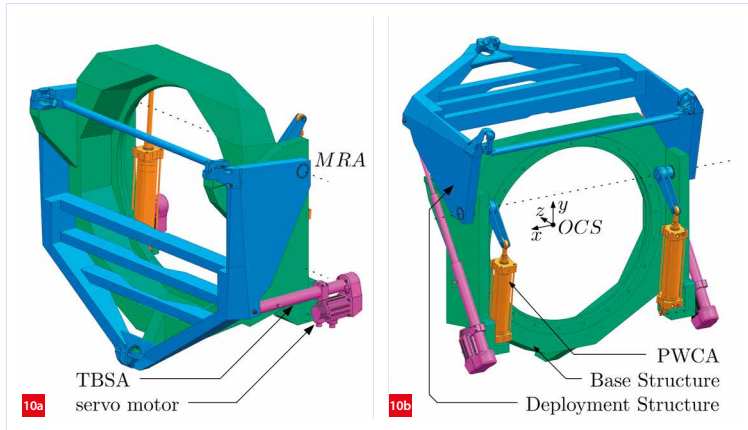
An elegant balance during deployment

The deployment and retraction of the mirror require rotation around the MRA, indicated by the dotted line in Figures 11a and 11b. Precise positional control during this rotation is provided by two Telescopic Ball-Screw Actuators (TBSAs), highlighted in pink, located symmetrically on either side of the structure.

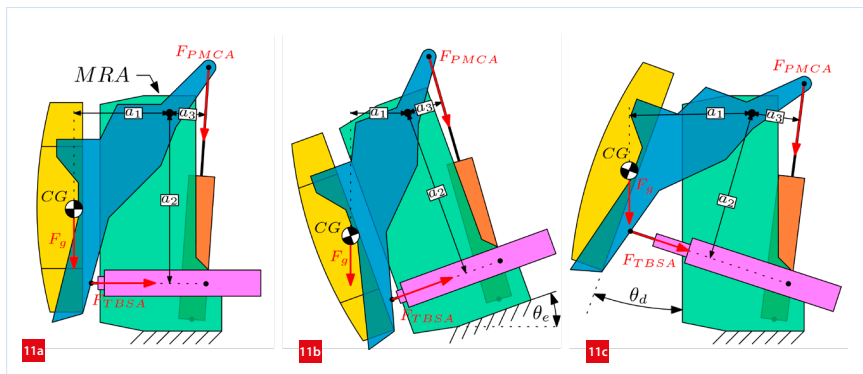
To ensure operational stability, the TBSA must remain under tension to prevent potential buckling from compression forces. Furthermore, maintaining radial preload on the MRA hinge bearings is essential to eliminate play at pivot points, thus preserving positional accuracy. Compensation using counter-balancing masses is not an option due to strict a mass constraint.

To tackle these challenges without adding counter-balancing mass, a system using a Pneumatic Weight Compensation

Actuator (PWCA) – comprising two pneumatic cylinders shown in orange – is implemented, as shown in Figure 10. During deployment and retraction, overcoming the gravitational force acting on the mirror is the primary mechanical



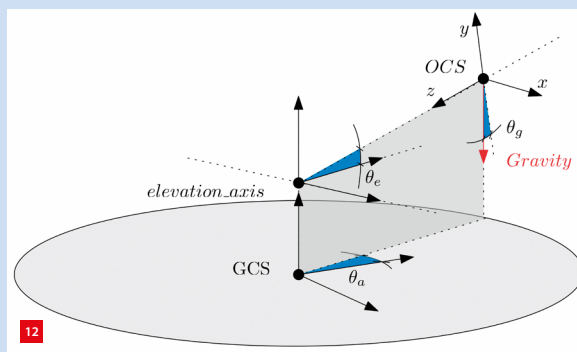
CAD model showing relevant components of the deployment mechanism. (a) Isometric front view of the deployed configuration. (b) Isometric rear view of the retracted configuration.



Free-body diagram illustrating orientation dependent on the deployment mechanism. (a) Deployed configuration while horizon pointing ($\theta_e = 0^\circ, \theta_d = 0^\circ$). (b) Deployed configuration while pointing on sky ($\theta_e = 20^\circ, \theta_d = 0^\circ$). (c) Intermediate configuration while horizon pointing ($\theta_e = 0^\circ, \theta_d = 20^\circ$).

Varying gravitational loads

The Keck II telescope can precisely target specific points in the sky by rotating around two axes, azimuth (θ_a) and elevation (θ_e), as shown in Figure 12. Azimuth rotation is perpendicular to the Earth’s surface, while elevation allows for horizon, zenith and intermediate pointing angles. The unit vectors of the telescope’s coordinate system (OCS) change in the Global Coordinate System (GCS) as the elevation angle shifts, causing the direction of the gravity vector within the OCS to change. At 0° elevation (horizon pointing), the gravity vector points in the negative y -direction, while at 90° elevation (zenith pointing), it points in the positive z -direction. At intermediate angles, the gravity vector forms a corresponding angle with the OCS xy -plane. The requirements state that elevation (θ_e) can be between 0° and 95° during operation of the telescope.



Keck II motion-axis definition including gravity vector (red), GCS, OCS, θ_a and θ_e .

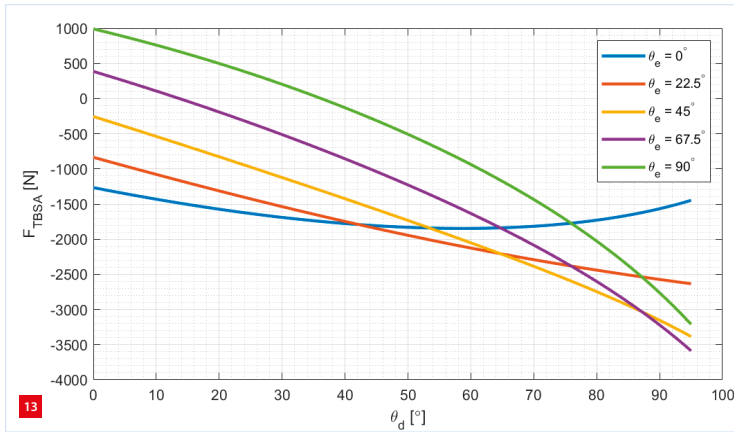
challenge. Although the gravitational force magnitude remains constant, its effective moment around the MRA varies significantly due to its changing direction, as explained in Figure 11 and the text box.

The telescope-elevation angle (θ_e) has an impact on the moment arm to which the gravitational force applies. This is indicated in the differing length of a_i between Figures 11a and 11b. Furthermore, changing the deployment angle (θ_d) has an effect on all moment arms, as illustrated by the length difference for a_1, a_2 and a_3 between Figures 11a and 11c. This yields significant nonlinear force-moment profiles over the full range of both θ_e and θ_d , leading to the conclusion that this cannot be compensated using a single spring element.

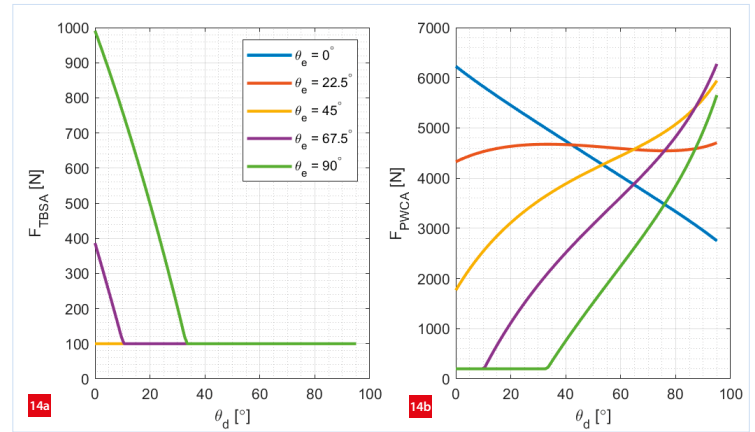
First, take a scenario without pneumatic weight compensation ($F_{PWSA} = 0$). Figure 13 shows the loading of the TBSA under varying combinations of θ_e and θ_d . These include undesirable compression forces of up to approximately 3,500 N and a problematic change in force direction. Both of which can lead to potentially significant deformation and play that subsequently result in loss of repeatability.

Activating the pneumatic weight-compensation system addresses this issue effectively. Pneumatic actuators allow adjustable force via pressure control. A carefully managed force profile is designed, which resulted in the TBSA operating exclusively under tension. Figure 14 illustrates a proposed balanced force profile over θ_d for both TBSA and PWCA at various telescope-elevation angles (θ_e).

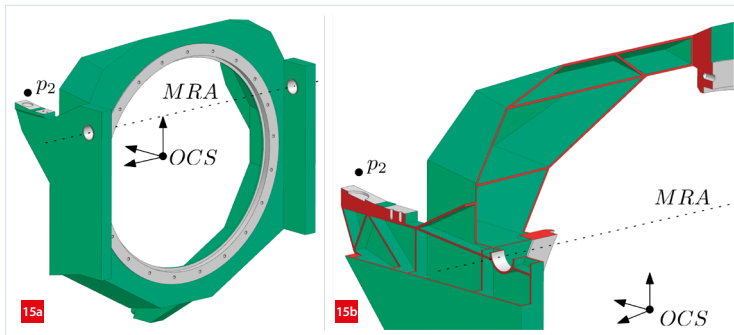
With this implementation, the TBSAs consistently experience a minimum tension force of 100 N, ensuring preload accounting for control-loop variations in pneumatic actuators. Additionally, PWCA forces remain in tension, optimised to operate effectively within the system’s maximum pressure specification of six bar.



Required TBSA actuation force over various elevation and retraction angles with inactive PWCA.



Result of the implementation of active PWCA.
 (a) Required actuation force by the TBSA with active PWCA.
 (b) Corresponding PWCA-applied force.



CAD model of Base Structure from multiple viewing angles.
 (a) Rear isometric view; all white highlighted faces are to be post-processed.
 (b) Section cut rear isometric view, with the thin aluminium plate structure clearly visible.

A light and stiff Base Structure

The Base Structure introduced in Figure 7 connects the flexible elements at points p_1 , p_2 and p_3 to the KWFI through the white ring illustrated in Figure 15. Additionally, it supports the bearing mounts at the MRA.

This Base Structure is a thin-walled welded assembly that creates a light and stiff structure. To mitigate thermal deformations due to the welding process, thicker pieces of material are implemented at critical interfaces, specifically at the connection points with the KWFI, the mirror mounts and the MRA bearings. These thicker sections are subsequently machined to specification, ensuring precise alignment and accurate positional tolerances.

An aluminium alloy is selected primarily for its low density combined with a specific stiffness comparable to steel, enabling the use of thicker plates without significantly increasing weight, thus enhancing structural eigenmodes. A similar construction strategy is used for the deployment structure.

Aluminium's relatively high coefficient of thermal expansion (CTE), as compared to steel or titanium, poses challenges for

maintaining alignment accuracy. However, the high thermal conductivity of aluminium results in low thermal gradients of the part. This allows mitigation of the thermal drift with refined open-loop control, using strategically placed thermocouples and the hexapod actuator system (introduced previously in Figure 3). With these measures, thermal errors impacting alignment were estimated to be effectively reduced to approximately 10% of their original magnitude.

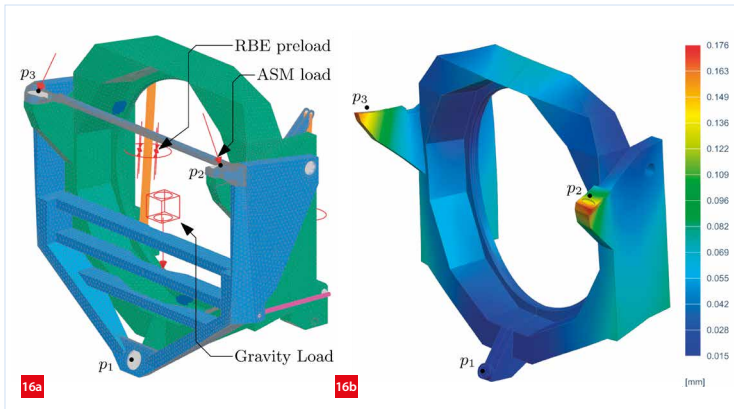
Structural analysis

The structural components of the validation model are analysed and optimised with the help of numerical calculations; see Figure 16. Here, Figure 16a shows the set-up of an analysis representing deployed horizon pointing, where the ASM is supported by the Base Structure (BS). As the ASM is exactly constrained to the BS through elastic elements, the forces acting on each of the three BS points p_1 , p_2 and p_3 can be calculated and applied directly. Note that in this specific loading condition, this resulted in a load only on p_1 and p_2 .

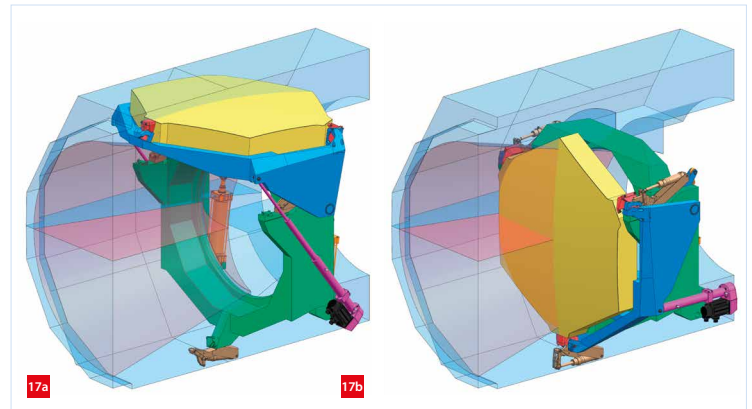
Additionally, a gravity load is applied to account for the weight of the structure itself. To define nodal points for additional load and constraint application, RBE3 elements (Rigid Body Element type 3) are used. These elements distribute loads among connected nodes without adding stiffness to the model, resulting in a conservative worst-case assumption. A bolt preload force is used to represent the force exerted by the PWCA between the Base Structure and the Deployment Structure. The displacement of each of the three points p_1 , p_2 and p_3 is obtained, which can be combined into a resulting displacement of the FSC.

Results

To summarise the findings, Figure 17 presents the final validation model within the partially cut-away design space,



Computational analysis of Base Structure; multiple additional components are implemented to assure realistic loading.
 (a) Numerical simulation set-up including loads and constraints.
 (b) Deformation magnitude plot, with the resulting gradient in mm.



Final CAD of the validation model.
 (a) Retracted configuration, full validation model additionally clears the KWFI light path.
 (b) Deployed configuration, full validation model keeps within the boundary volume.

Table 1
 Predicted stability of the ASM Face Sheet Centroid based on the final validation model.

Error source	x [μm]	y [μm]	z [μm]	Rx [μrad]	Ry [μrad]	Rz [μrad]
Gravitational	0.00	5.22	1.92	1.07	0.00	0.00
Thermal	0.00	0.18	5.32	0.62	0.00	0.00
Aerodynamic	8.19	3.19	0.55	0.83	0.48	3.31
Stability realised (±)	12.94	13.90	10.90	8.31	4.40	8.35
Stability budgeted (±)	46	46	7	34	34	280

as introduced in Figure 6. The results demonstrate that, in terms of spatial feasibility, implementing a deployable system that functions at all telescope angles is geometrically viable with an ASM thickness of 228 mm.

Based on additional numerical simulations and analytical calculations of all influential components – which account for gravitational, thermal and aerodynamic forces – as well as the compensation capabilities of the hexapod and analytical calculations of virtual play in all rotating and sliding components, the total resulting analytical stability error is determined; see Table 1.

This results in all positional requirements being reached except the one for the z-position. Most of this error, however, is due to thermal deformation. If the structure were to feature more thermocouples, a better open-loop model for active compensation is expected to result in a pass.

Conclusion

The result of this work proves the feasibility of a deployable ASM employed in the Keck II telescope. The design’s light and stiff aluminium-plate structure provides structural integrity. Deployment stability and repeatability are achieved through a flexible Maxwell mount, a confidential

deployment mechanism and an active thermal compensation system. Telescopic ball-screw actuators, supported by pneumatic weight compensation, facilitate deployment at every telescope-elevation angle.

Besides the undiscussed confidential repeatability mechanism, the research into the feasibility of using carbon-fibre reinforced plastics in the ASM itself [4] has also not been presented here. In March 2025, TNO won its bid to develop the stationary ASM [6].

REFERENCES

[1] W.M. Keck Observatory, “Keck 2035 Strategic Plan”, 2024, accessed Apr. 4, 2025, www.keckobservatory.org/wp-content/uploads/2024/05/Keck2035_StratPlan.pdf
 [2] J. Prochaska, et al., “Keck 1 deployable tertiary mirror (K1DM3)”, in *SPIE Astronomical Telescopes + Instrumentation*, Amsterdam (NL), 2012.
 [3] M. Radovan, et al., “Conceptual design of the Keck Wide Field Imager (KWFI)”, in *Ground-based and Airborne Instrumentation for Astronomy IX*, Montréal (Canada), 2022.
 [4] B. Huisman, “Architectural Design of a Deployment Mechanism for the Keck II Telescope’s Adaptive Secondary Mirror, Including Research Into the Implications of Using CFRP for its Backing Structure”, M.Sc. thesis, Eindhoven University of Technology, 2023.
 [5] J. Maxwell, “General Considerations Concerning Scientific Apparatus”, *The Scientific Papers of James Clerk Maxwell*. New York (NY, USA), Dover Press, 1890, pp. 19, 68.
 [6] TNO, “TNO technology selected for Secondary Mirror of W. M. Keck Observatory”, accessed Apr. 4, 2025, www.tno.nl/en/newsroom/2025/02/tno-technology-selected-secondary-mirror.